Dynamic Systems and Applications 18 (2009) 129-142

AN EFFECTIVE SEMI-IMPLICIT METHOD FOR CIRCULARLY SYMMETRIC QUENCHING OPTICAL WAVES

QIN SHENG

Center for Astrophysics, Space Physics & Engineering Research, Department of Mathematics, Baylor University, Waco, TX 76798-7328
(Qin_Sheng@baylor.edu)

ABSTRACT. Recent electro-optical studies indicate that the spatial profile of a quenching, or collapsing, optical wave evolves to a specific circularly symmetric shape, known as the Townes profile, for elliptically shaped or randomly distorted input beams. Computations of such a Townes profile have been playing an important role in understanding of the wave collapse phenomenon, but the numerical procedures are sensitive due to features of the generalized nonlinear Schrödinger equation boundary value problems involved. This paper studies an effective semi-implicit finite difference method equipped with a dynamic shooting strategy for the numerical solution of the quenching optical boundary value problems. The numerical method proposed is simple in structure, easy to use, and weakly asymptotically stable. Simulated circularly symmetric quenching optical waves are given.

Keywords: Self-similarity, quenching wave, optical beams, shooting method, consistency, stability, convergence, boundary and initial values

AMS (MOS) Subject Classification: 34A45, 39A13, 74H15, 74S20

1. INTRODUCTION

Quenching or collapse of a wave due to nonlinearity in the system is an ubiquitous phenomenon spanning many fields of science and engineering. It has been important, especially in the study of negative index materials [8, 12, 19]. Recently a self-similar shape was identified as an intense optical pulse collapses in a nonlinear medium due to [3–5, 7, 9, 15–18]. The form of an optical pulse propagating through glass as it collapses fits the so-called Townes profile, which is numerically extracted as a stationary solution of the radially symmetric, two-dimensional nonlinear Schrödinger equation. Thus, even though the Townes profile is unstable, it still dictates the beam shape during collapse [11]. The universality of the self-similar Townes profile shapes has not been established under general conditions, since the profiles may be difficult to generate in the unstable situations that are sometimes encountered in the experiments. In this paper an efficient and effective numerical method is presented

The research was supported in part by a VPR research grant from the Baylor University under No. 032-1318-06.

to accurately generate the stationary solutions, whether they are stable or unstable, to the nonlinear Schrödinger equation suitable for general forms of the nonlinearity [6, 15, 16].

We consider the two-dimensional generalized nonlinear Schrödinger equation

$$2ikU_z + U_{xx} + U_{yy} + \frac{2k^2 n_2}{n_0} f(|U|)U = 0, \tag{1.1}$$

where U represents the amplitude of the electric field, $k = 2n_0\pi/\lambda$ is the propagation wave vector, λ is the vacuum wavelength, $n_0,\ n_2$ are the linear and nonlinear indexes of refractions, respectively, and z is the wave propagation direction. While $U_{xx} + U_{yy}$ represents the wave diffraction involved, the nonlinear term in (1.1) accounts for the intensity-dependent refractive index $n = n_0 + n_2\phi$, where $\phi = |U|^2$ is the intensity and contributes to self-focusing [6, 7, 12]; the nonlinear term of the refractive index is called as Kerr nonlinearity. The function f to be used is $f(\xi) = \xi^2/(1+\xi^2)$, which describes a nonlinear median with a saturable nonlinearity [4, 5, 10]. Removing U_{yy}, equation (1.1) is well-known for its integrability and analytical existence of the one-dimensional soliton. While the solitary solutions still exist in higher dimensional cases, they are often unstable to small perturbations. The pulses obtained corresponding to the Kerr nonlinear function may either delocalize or undergo collapse depending on the initial conditions (see [3, 4, 8, 10] for more details). In the saturable median, the nonlinear focusing and diffraction precisely balance each other, and the beam maintains a constant profile [12, 16]. We further consider the following boundary conditions for (1.1),

$$U_x(0, y, z) = 0,\ U_y(x, 0, z) = 0,\ \lim_{|x|+|y|\to\infty} U = 0. \tag{1.2}$$

Denote $r = \sqrt{x^2 + y^2}$. In a locally circularly symmetric environment, all waveguide solutions of (1.1), (1.2) can be written as

$$U = \sqrt{\frac{n_0}{2k^2 n_1}} e^{i\alpha^2 z/2k} u_\alpha(r),$$

where $\alpha > 0$ is an arbitrary constant, $u_\alpha = \alpha u(\alpha r)$, and $u(r)$ satisfies the following dimensionless boundary value problem [3, 10, 12]:

$$u'' + \frac{1}{r}u' - \beta u + f(u)u = 0,\ r > 0, \tag{1.3}$$

$$u'(0) = 0,\ \lim_{r\to\infty} u(r) = 0, \tag{1.4}$$

where β depends on α. Among the solutions of (1.3), (1.4), we are particularly interested in the sequence of so-called *nth mode quenching profiles* $R_n(r)$ which has exactly n positive roots for any nonnegative integer n. Solutions $R_n(r),\ n = 0, 1, 2, \ldots$, play a central role in nonlinear optical wave collapses and the intensity profile in circularly symmetric environments [6, 12, 17].

Due to the importance and difficulties in obtaining $R_n(r)$ analytically, various kinds of numerical methods have been developed for approximating the nth mode quenching profiles. Most existing simulation results are for n up to 3, and only with relatively small r intervals used, however.

On the other hand, in recent numerical explorations, we noticed that the convergence of the numerical solutions R_n with large n values are extremely slow via conventional shooting schemes, especially when large r intervals are used. These motivate us for a practically simple, more efficient and effective method. We will concentrate on the circularly cases (1.3), (1.4), and the investigations can be extended to general cases including (1.1), (1.2) based on wave similarities.

This paper is organized as follows. In the next section, our semi-implicit finite difference method utilizing uniform and nonuniform meshes will be presented. A simple but effective grid adaptation for deriving a nonuniform mesh will be introduced via an arc-length monitoring function. Then, in Section 3, we will show that the schemes are consistent and weakly asymptotically stable [1, 9, 11, 13]. A dynamic shooting strategy which offers a fast and robotic convergence procedure for the solution sequences will be generated. In Section 4, we will carry out a series of simulation experiments. Computed intensity profiles will be presented in two and three dimensional fashions, respectively. Sequences of initial value approximations will be given to illustrate the fast convergence. Results obtained are consistent with known experimental predictions [4, 12, 16, 18]. Brief conclusion and remarks will be given in Section 5.

2. SEMI-IMPLICIT FINITE DIFFERENCE SCHEME

Since the quenching profile locates extensively within the region near the origin, naturally, we let $[0, M]$ be the interval interested, $M \gg 0$, and let $\Omega = \{r_0, r_1, \ldots, r_{N+1};\ r_0 = 0,\ r_{N+1} = M\}$ be a mesh superimposed upon the interval. Denote $r_{k+1} - r_k = h_k,\ k = 0, 1, \ldots, N$. We say that Ω is *uniform* if $h_k \equiv h > 0$ for all k, otherwise Ω is *nonuniform* [2]. Let u_k be an approximation of $u(r_k)$, the solution of (1.3), (1.4) at r_k.

We introduce the following *nonstandard semi-implicit scheme*:

$$\frac{2}{h_k + h_{k-1}}\left(\frac{u_{k+1} - u_k}{h_k} - \frac{u_k - u_{k-1}}{h_{k-1}}\right) + \frac{1}{r_{k+1} + r_{k-1}}\left(\frac{u_{k+1} - u_k}{h_k} + \frac{u_k - u_{k-1}}{h_{k-1}}\right)$$

$$-\beta u_k + f(u_k)u_k = 0,\ k = 1, 2, \ldots, N-1. \tag{2.1}$$

It is not difficult to verify that when Ω is uniform, the above scheme reduces to a *standard semi-implicit scheme*:

$$\frac{u_{k+1} - 2u_k + u_{k-1}}{h^2} + \frac{u_{k+1} - u_{k-1}}{h(r_{k+1} + r_{k-1})} - \beta u_k + f(u_k)u_k = 0,\ k = 1, 2, \ldots, N-1. \tag{2.2}$$

Schemes (2.1) and (2.2) are consistent with (1.3) [14, 15]. The scheme (2.1) is first order accurate while (2.2) is second order accurate.

We divide the shooting procedure into several rounds, and each round consists of a sequence of shootings. To compute $R_n(r)$, in the j-th round, $j \geq 1$, we start with a pair of estimated initial values $R_{n,j,0}(0)$ and $R_{n,j,L}(0)$ with $R_{n,j,0}(0) < R_{n,j,L}(0)$, where $L > 0$ is sufficiently large. $R_{n,j,0}(0)$ serves as the *starting initial value* while $R_{n,j,L}(0)$ is the *terminating initial value* in the round of shootings for $R_n(r)$. The initial pair of such $R_{n,1,0}(0),\ R_{n,1,L}(0)$ may be selected via either a random search or a testing experiment. For the sake of brevity, we start with $j = 1$. The proposed computational procedure can be stated as:

Step 1: Let $L \gg 0$. Choose the initial value pair $R_{n,1,0}(0),\ R_{n,1,L}(0)$.

Step 2: Compute the shooting step size

$$\tau_{n,1} = (R_{n,1,L}(0) - R_{n,1,0}(0))/L. \tag{2.3}$$

Step 3: Set a sequence of initial conditions for (2.2) or (2.1):

$$R_{n,1,k}(0) = R_{n,1,k}(0),\ R'_{n,1,k}(0) = 0,\ k = 0, 1, 2, \ldots, L, \tag{2.4}$$

where

$$R_{n,1,k}(0) = R_{n,1,k-1}(0) + \tau_{n,1},\ k = 1, 2, \ldots, L-1. \tag{2.5}$$

Calculate the corresponding numerical solutions $R_{n,1,k}(r),\ k = 0, 1, 2, \ldots, L$, via either of the schemes established.

Step 4: The sequence of computations may terminate at its maturity, that is, $k = L$, or once a stopping criterion is satisfied. We will determine if any of the shootings offers a satisfactory solution, or we may select the last two values from $\{R_{n,1,k}(0)\}_{k=0}^{K}$, $K \leq L$, to be the new pair of initial values, $R_{n,2,0}(0)$ and $R_{n,2,L}(0)$, $R_{n,2,0}(0) < R_{n,2,L}(0)$, for the next round of shooting operations. Steps 2-4 will be repeated till a satisfactory approximation of $R_n(r)$ is reached.

We suggest the following simple but effective stopping criteria:

SC$_1$.: Let $\|\cdot\|$ be an Euclid norm. We compare the numerical solution at the kth stage of jth round, that is, $\|R_{n,j,k}(r)\|$, and a theoretically predicted value $\|R_n(r)\|$. The shooting stops as soon as the relative error of $\|R_{n,j,k}(r)\|$ is less than a tolerance ϵ:

$$\frac{|\|R_{n,j,k}(r)\| - \|R_n(r)\||}{\|R_n(r)\|} < \epsilon,\ 0 \leq k \leq L.$$

SC$_2$.: Exam the function values of $R_{n,j,k}(r)$ and see if they are sufficiently small for a set of sufficiently large $r \in \Omega$. That is, for sufficiently large ℓ_1 and ℓ_2, if we

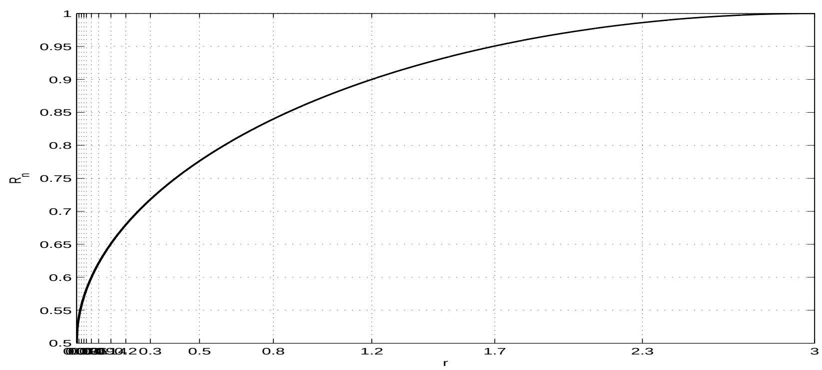

FIGURE 1. An illustration of the nonuniform mesh based on ellipses. $M = 3$ and the number of grids $N = 15$ are used.

have

$$\sum_{\ell=\ell_1}^{\ell_2} |R_{n,j,k}(r_\ell)| \le \epsilon,\ 0 \le k \le L,$$

for given $\epsilon > 0$.

SC$_3$.: Check whether the inequality, $R_{n,j,k}(r_p)R_{n,j,k+1}(r_p) < 0,\ 0 \le k < L$, is true at a carefully selected testing point r_p, $0 < p < N$. The inequality indicates a change of the solution pattern and a restart of the shooting algorithm may have become necessary. The criterion works particularly well and reliably in our simulation procedures.

SC$_4$.: The computation terminates if

$$\tau_{n,j} < \epsilon,\ j \ge 1,$$

is reached for given $\epsilon > 0$.

In summary, to compute the numerical approximation of $R_n(r)$, in each round of shooting operations, we start with a pair of predetermined initial value pair. The sequence of computations is then conducted under the initial conditions

$$R_{n,j,k}(0) = R_{n,j,k}(0),\ R'_{n,j,k}(0) = 0,\ j = 1, 2, \ldots;\ k = 0, 1, 2, \ldots, L,$$

where

$$R_{n,j,k}(0) = R_{n,j,k-1}(0) + \tau_{n,j},\ j = 1, 2, \ldots;\ k = 1, 2, \ldots, L-1,$$

with $\tau_{n,j} = (R_{n,j,L}(0) - R_{n,j,0}(0))/L$. Except the initial pair of values, $R_{n,1,0}(0)$ and $R_{n,1,L}(0)$, the rest pairs of starting initial values are determined by the previous round of shooting computations. This simple procedure remarkably improves the convergence of the initial value value sequence for a successful shooting method.

Although a more rigorous numerical analysis is needed for the convergence, our experiments have been overwhelmingly successful. Numerical results shown in the next section have demonstrated both fast convergence and numerical stability of the schemes.

To achieve a higher order accuracy, finer steps $h,\ h_k$ are often required. Recall the fact that our interval $[0, M]$ used is large. Therefore larger systems may result as a consequence of higher accuracy. This may significantly reduce the efficiency of computations. On the other hand, we may notice that the oscillatory nonlinear activities corresponding to the Townes profile occur only in areas close to the origin. Therefore, it is not necessary to do the refinement throughout the entire domain. A standard arc-length adaptation may be too costly here, since shapes of the shooting solutions change rapidly during computations. To balance the simplicity, accuracy and effectiveness of the nonuniform meshes without calculating exactly the arc-lengths of nth mode solutions, we propose an ellipse based nonuniform mesh centered at $(M, 1/2)$ with a major axis of M in the r direction and a minor axis of $1/2$ in the $u = R_n(r)$ direction, as shown in Figure 1. An equidistribution formula then be introduced [2, 13, 14]:

$$h_k = \frac{Mh}{2C}\left[1 + \sqrt{1 - \frac{(x_k - M)^2}{M^2}}\ \right],\ k = 1, 2, \ldots, N,$$

where $x_k = kh,\ h = C/N$ is the *mathematical step size* and C is the quarter of the elliptic arc-length as $0 \le r \le M,\ 0 \le u \le 1/2$. Distribution of variable *physical steps* can thus be conveniently calculated on $[0, M]$, no matter how big M is.

The nonuniform meshes turn out to be very successful in our simulations. We will continue to optimize the grid distribution by employing other featured curves other than ellipses for the basic setting.

3. STABILITY OF THE NUMERICAL METHOD

Here we prove the stability of two forms of the nonlinear equations. Let $F(u) = 0$ be a nonlinear differential equation defined on $[0, M]$ and

$$G(v) = \sum_{j=k-m}^{k+n} \alpha_j v_j = 0 \tag{3.1}$$

be a semi-implicit finite difference scheme defined on Ω, where α_j may depend on $v_{k-m},\ v_{k-m+1},\ \ldots,\ v_{k+n-1}$. Denote $\tilde{h} = \max_k h_k$. Based on [15, 16], we have

Definition 3.1. We say that G is a consistent approximation to F if

$$F(w) - G(w) = O(\tilde{h}^{\kappa}),\ \kappa > 0,$$

where w is a sufficiently smooth function defined on $[0, M]$. Further, we say that G is of order κ in approximation if it is consistent.

Definition 3.2. Let

$$\sum_{\ell=k-m}^{k+n} \alpha_j \rho^j = 0$$

be corresponding stability polynomial of (3.1) and Φ be the set of its roots. We say that the semi-implicit difference scheme (3.1) is weakly asymptotically stable if

$$\max_{\rho\in\Phi}|\rho| = O(1)$$

as $\tilde{h}\to 0$.

We may prove the weakly asymptotical stability of the schemes (2.2), (2.1).

Theorem 3.1. *The uniform scheme* (2.2) *is weakly asymptotically stable with* $f(\xi) = \xi^2/(1+\xi^2)$.

Proof. Let $u_k = \rho^k,\ \rho\neq 0$. Substitute it into (2.2). Simplifying the expressions, we obtain

$$\frac{\rho^2-2\rho+1}{h^2} + \frac{\rho^2-1}{h(r_{k+1}+r_{k-1})} - \beta\rho + \frac{\rho\rho^{2k}}{1+\rho^{2k}} = 0.$$

This yields the following quadratic equation:

$$\left(\frac{1}{h^2}+\frac{1}{h(r_{k+1}+r_{r-1})}\right)\rho^2 - \left(\frac{2}{h^2}+\beta-\frac{\rho^{2k}}{1+\rho^{2k}}\right)\rho + \frac{1}{h^2} - \frac{1}{h(r_{k+1}+r_{k-1})} = 0.$$

Solve the above equation, we acquire a pair of roots

$$\begin{aligned}
\rho &= \frac{\frac{2}{h^2}+P\pm\sqrt{\left(\frac{2}{h^2}+P\right)^2-4\left(\frac{1}{h^4}-\frac{1}{h^2(r_{k+1}+r_{k-1})^2}\right)}}{2\left(\frac{1}{h^2}+\frac{1}{h(r_{k+1}+r_{k-1})}\right)}\\
&= \frac{2+h^2P\pm\sqrt{\left(2+h^2P\right)^2-4\left(1-Q^2\right)}}{2\left(1+Q\right)}\\
&= \frac{1+\frac{h^2P}{2}\pm\sqrt{h^2P+\left(\frac{h^2P}{2}\right)^2+Q^2}}{1+Q}, \qquad (3.2)
\end{aligned}$$

where

$$P = \beta - \frac{u_k^2}{1+u_k^2},\ Q = \frac{h}{r_{k+1}+r_{k-1}}.$$

Note that for the rational function $s(\xi) = \xi/(1+\xi),\ \xi > 0$, we have $s'(\xi) = 1/(1+\xi)^2 > 0,\ \xi > 0$. Therefore s is monotonically increasing and this indicates that $0 < s(\xi) < 1$ for $\xi > 0$. On the other hand, for the scaling parameter β we have $0 < \beta \le 1$ [2-4, 16]. These indicate that

$$-1 \le P \le 1.$$

And further, due to the fact that $r_{k+1}+r_{k-1} \ge 2h$, we have

$$0 < Q \le \frac{1}{2}.$$

Combining the above inequalities for (3.2), we find that

$$\lim_{h\to 0}\rho = \frac{1+Q}{1+Q} = 1.$$

Therefore the difference scheme discussed is weakly asymptotically stable. □

Theorem 3.2. *The nonuniform scheme* (2.1) *is weakly asymptotically stable with* $f(\xi) = \xi^2/(1+\xi^2)$.

Proof. Since Ω is nonuniform, we let $u_k = \prod_{j=1}^{k} \rho_j$, $\rho_j \neq 0$, for (2.1). After the substitution and a straightforward simplification, we observe that

$$\begin{aligned}
&\frac{2}{h_k + h_{k-1}} \left(\frac{\rho_{k+1}\rho_k - \rho_k}{h_k} - \frac{\rho_k - 1}{h_{k-1}} \right) \\
&+ \frac{1}{r_{k+1} + r_{k-1}} \left(\frac{\rho_{k+1}\rho_k - \rho_k}{h_k} + \frac{\rho_k - 1}{h_{k-1}} \right) - \tilde{P}\rho_k = 0, \; k = 1, 2, \ldots,
\end{aligned} \tag{3.3}$$

where

$$-1 < \tilde{P} = \beta - \frac{u_k^2}{1 + u_k^2} < 1.$$

Now, recall the necessary smoothness constraints for nonuniform adaptive grids [1, 6, 14, 15], we must require that

$$ph_k \le h_{k+1} \le qh_k,$$

where $q = O(p)$ and $q \ge p > 0$. Hence, without loss of generality, we may assume that $h_k = ah_{k-1} = ah$, $\rho_{k+1} = b\rho_k = b\rho$, where $0 < a,\ b \le 1$ are two constants. A substitution of these relations into (3.3) yields

$$\begin{aligned}
&\frac{2}{(1+a)h} \left(\frac{b\rho^2 - \rho}{ah} - \frac{\rho - 1}{h} \right) + \frac{1}{r_{k+1} + r_{k-1}} \left(\frac{b\rho^2 - \rho}{ah} + \frac{\rho - 1}{h} \right) - \tilde{P}\rho = 0, \\
&\qquad k = 1, 2, \ldots
\end{aligned}$$

The above can be rearranged to generate the following identity:

$$\begin{aligned}
&\frac{b}{ah} \left(\frac{2}{(1+a)h} + \frac{1}{r_{k+1} + r_{k-1}} \right) \rho^2 \\
&- \frac{1}{h} \left[\frac{2}{(1+a)h} \left(1 + \frac{1}{a} \right) + \tilde{P}h - \frac{1}{r_{k+1} + r_{k-1}} \left(1 - \frac{1}{a} \right) \right] \rho \\
&+ \frac{1}{h} \left(\frac{2}{(1+a)h} - \frac{1}{r_{k+1} + r_{k-1}} \right) = 0.
\end{aligned}$$

It follows therefore the following quadratic equation must be true:

$$\frac{b}{a} \left(\frac{2}{1+a} + Q \right) \rho^2 - \left[\frac{2}{1+a} \left(1 + \frac{1}{a} \right) + \tilde{P}h^2 - Q \left(1 - \frac{1}{a} \right) \right] \rho + \frac{2}{1+a} - Q = 0,$$

for which we may obtain

$$\rho = \frac{2 + a\tilde{P}h^2 + (1-a)\,Q \pm R}{2b\left(\frac{2}{1+a} + Q\right)}, \tag{3.4}$$

where the quantity

$$R = \sqrt{\left[2 + a\tilde{P}h^2 + (1-a)\,Q\right]^2 - 4ab\left(\frac{4}{(1+a)^2} - Q^2\right)}.$$

Based on the boundedness of the functions $\tilde{P}$, Q, we conclude readily that

$$\rho = O(1) \text{ as } h \to 0,$$

and thus the scheme investigated is weakly asymptotically stable for any fixed nontrivial constants a and b. □

4. SIMULATION RESULTS

Our numerical experiments are carried out with β values varying from 0.010 to 0.999. The speed of convergence of the shooting sequences is satisfactory and the numerical solutions are of great interests. Without loss of generality, we fix the variables $L = 100$, $M = 64$ and $N = 6057$ throughout our demonstrations, where N is the maximal number of grids in Ω. These lead to $h = 0.10566$ for the uniform mesh; and $h = C/N = 0.013278$ as the mathematical step size for the variable nonuniform mesh, since the elliptic arc-length $C \approx 80.430155$. Let J be the maximal number of rounds executed. Unless otherwise declared, Stopping Criteria SC_3 and SC_4 are adopted. For the purpose of comparison, we only show numerical results $R_0(r)$, $R_1(r)$, $R_2(r)$, $R_3(r)$, in particular $R_3(r)$, obtained via (2.1) on nonuniform grids. Computations of higher mode $R_n(r)$ are similar. Double precision floating point arithmetic is used on Dell Precision 670 computer platforms. Fortran 90 and MatLab subroutines are used in the experiments. Values of the scaling parameter $\beta = 0.5$ is used in simulations.

Computed results are verified with known results [12, 16, 18]. Three-dimensional plots of the extended solution u_n corresponding to (1.3), (1.4) are given in Figures 2-5.

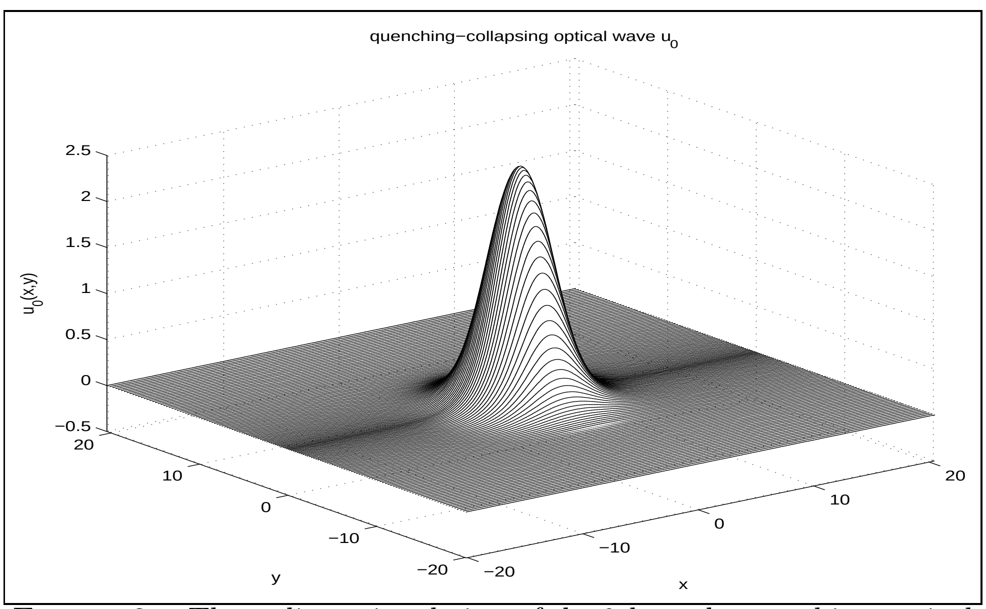

FIGURE 2. Three-dimensional view of the 0th mode quenching optical wave $u_0(x, y)$ generated through the profile $R_0(r)$.

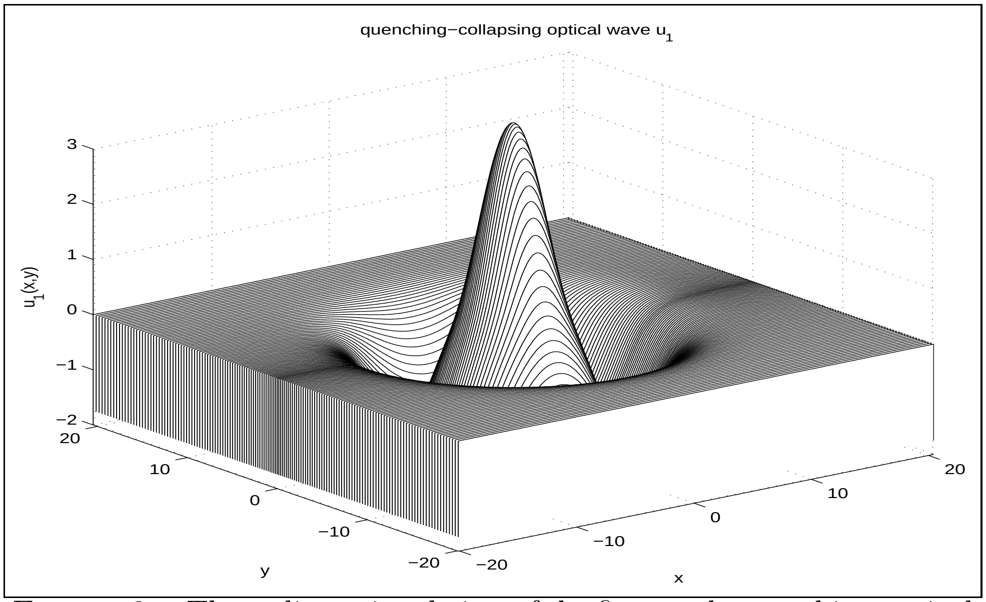

FIGURE 3. Three-dimensional view of the first mode quenching optical wave $u_1(x, y)$ generated through the profile $R_1(r)$.

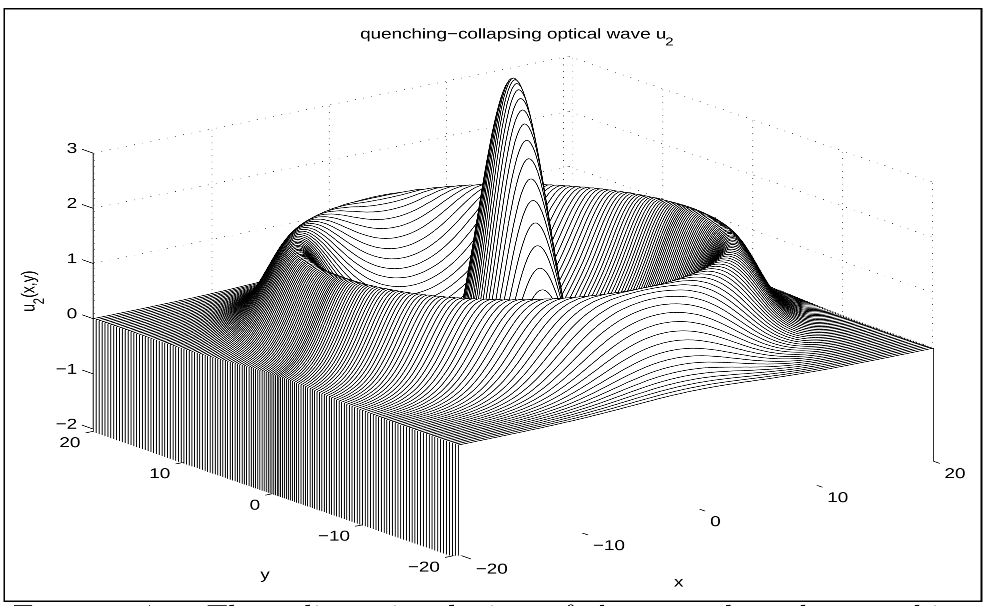

FIGURE 4. Three-dimensional view of the second mode quenching optical wave $u_2(x, y)$ generated through the profile $R_2(r)$.

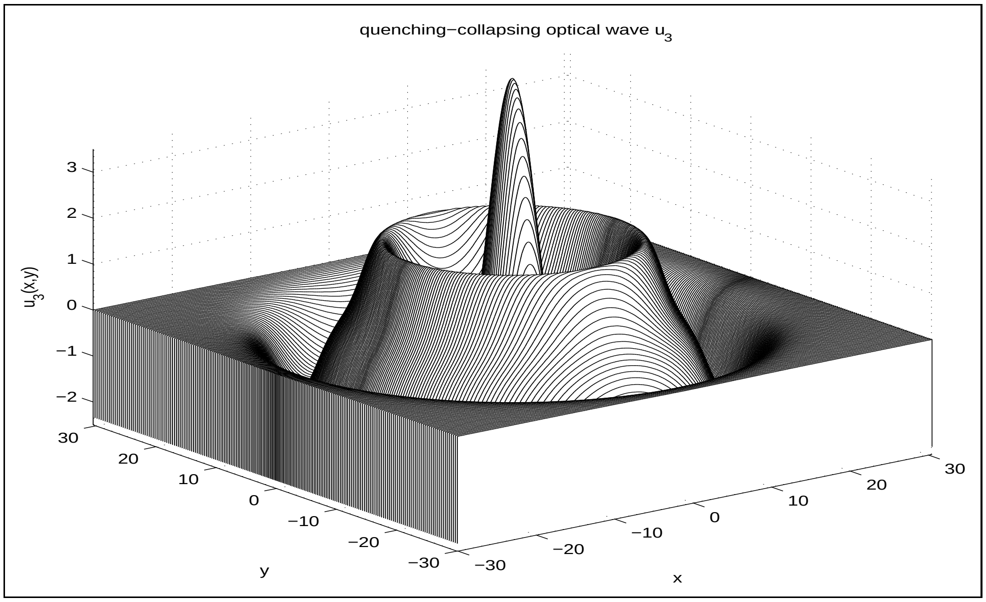

FIGURE 5. Three-dimensional view of the third mode quenching optical wave $u_3(x, y)$ generated through the profile $R_3(r)$.

5. CONCLUSION AND REMARKS

A family of two semi-implicit finite difference schemes equipped with a dynamic shooting procedure for quenching optical waves are developed and studied. We carried out the simulations on a version of the nonlinear Schrödinger equation with a saturable nonlinearity. The numerical algorithms are weakly asymptotically stable, and offer superior quality in convergence. The dynamic shooting strategy developed utilizes pairs of initial guesses instead one value in conventional methods. A practical adaptive mesh is introduced to achieve the simplicity of the method, while improving the efficiency in approaching $R_n(r)$ in a relatively large interval of r. The overall simulation procedures are simple, reliable and practically useful.

The use of different scaling factor values do not significantly affect the convergence of the semi-implicit method. Although when $\beta \to 1$, the convergence to $R_n(r)$ slows down due to the large amplitudes of peak values of the solutions encountered.

The nonphysical solutions are eliminated effectively during the rounds of shooting procedures. These may exhibit a particular monotone pattern which needs to be further investigated. Higher mode number solutions $R_n(r),\ n \geq 4$, can be computed similarly. However, the convergence is slightly slower in our simulations if large intervals of r are considered. We have also found stationary solutions for the Kerr nonlinear median; even though they are unstable. However, as pointed out in [11], those unstable solutions leave an impact on the quenching wave's final profile.

Similar ideas of the semi-implicit nonlinear schemes may be implemented for solving the generalized nonlinear Schrödinger equation problem (1.1), (1.2) in non-symmetric cases. Semi-discretization in space, or the method of lines, is a way to approach. The continuing study of the cases has been in good progress.

Acknowledgement

The author would like to thank the Office of Vice Provost on Research, Baylor University, for the generous support through a 2006-2007 VPR research grant under No. 032-1318-06. The author would like also to thank Dr. Joseph Haus, Director of the Electro-Optics Program at University of Dayton, for his wonderful discussions and encouragements throughout this study.

REFERENCES

[1] P. Benard, R. Laprise, J. Vivoda and P. Smolikova, The stability of semi-implicit schemes for the hydrostatic primitive equations systems for the fully elastic system of Euler equations: flat-terrain case, *Monthly Weather Review,* **132** (2004), 1306-1318.

[2] H. Cheng, P. Lin, Q. Sheng and R. C. E. Tan, Solving degenerate reaction-diffusion equations via variable step Peaceman-Rachford splitting, *SIAM J. Scientific Computing,* **25** (2003), 1273-1292.

[3] R. Y. Chiao, E. Garmire and C. H. Townes, Self-trapping of optical beams, *Phys. Rev. Lett.,* **13** (1964), 479-490.

[4] V. Dhayalant, T. Standnes, J. J. Stamnet and H. Heier, Scalar and electromagnetic diffraction point-spread functions for high-NA microlenses, *Pure Appl. Opt.,* **6** (1997), 603-615.

[5] A. Dubietis, E. Gaižauskas, G. Tamošauskas and P. Di Trapani, Light filaments without self-channeling, *Physical Review Letters,* **92** (2004), 253903/1-4.

[6] D. E. Edmundson, Unstable higher modes of a three-dimensional nonlinear Schrödinger equation, *Physical Review E,* **55** (1997), 7636-7644.

[7] A. Gürtler, C. Winnewisser, H. Helm and P. U. Jepsen, Terahertz pulse propagation in the near field and the far field, *J. Opt. Soc. Am. A,* **17** (2000), 74-83.

[8] B. J. Justice, J. J. Mock, L. Guo, A. Degiron, D. Schurig and D. R. Smith, Spatial mapping of the internal and external electromagnetic fields of negative index metamaterials, *Optics Express,* **14** (2006), 8694.

[9] R. Keppens 1, G. Tóth, M. A. Botchev and A. Van Der Ploeg, Implicit and semi-implicit schemes: algorithms, *Intern. Numer. Meth. Fluids,* **30** (1999), 335-352

[10] Y. S. Kivshar and G. P. Agrawal, *Optical Solitons from Fibers to Photonic Crystals,* Academic Press, 2003.

[11] M. Kolesik, E. M. Wright and J. V. Moloney, Dynamic nonlinear X waves for femtosecond pulse propagation in water, *Physical Review Letters,* **92** (2004), 253901/1-4.

[12] K. D. Moll, A. L. Gaeta and G. Fibich, Self-similar optical wave collapse: observation of the Townes profile, *Physical Review Letters,* **90** (2003), 203902/1-4.

[13] Q. Sheng and H. Cheng, An adaptive grid method for degenerate semilinear quenching problems, *Computers Math. Appl.,* **39** (2000), 57-71.

[14] Q. Sheng and A. Khaliq, Linearly implicit adaptive schemes for singular reaction-diffusion equations, Chapter 9, *Adaptive Method of Lines,* Chapman & Hall/CRC, London and New York, 2001, 263-294.

[15] Q. Sheng, A. Khaliq and E. Al-Said, Solving the generalized nonlinear Schrödinger equation via quartic spline approximation, *J. Comput. Physics,* **166** (2001), 400-417.

[16] J. M. Soto-Crespo, D. R. Heatley, E. M. Wright and N. N. Akhmediev, Stability of the higher-bound states in a saturable self-focusing medium, *Physical Review A,* **44** (1991), 636-644.

[17] C. Sulem and P.-L. Sulem, *Nonlineaar Schrödinger Equations: Self-focusing and Wave Collapse,* Springer, London and New York, 1999.

[18] P. Di Trapani, G. Valiulis, A. Piskarskas, O. Jedrkiewicz, J. Trull, C. Conti and S. Trillo, Spontaneously generated X-shaped light bullets, *Physical Review Letters,* **91** (2003), 093904/1-4.

[19] J. Yang, Internal oscillations and instability characteristics of (2+1)-dimensional solitons in a saturable nonlinear medium, *Physical Review E,* **66** (2002), 026601/1-9.